

Total Coloring and Efficient Domination Applications to Non-Cayley Non-Shreier Vertex-transitive Graphs

Italo J. Dejter^{1,✉}

¹ *University of Puerto Rico Rio Piedras, PR 00936-8377*

ABSTRACT

Let $0 < k \in \mathbb{Z}$. Let the star 2-set transposition graph ST_k^2 be the $(2k - 1)$ -regular graph whose vertices are the $2k$ -strings on k symbols, each symbol repeated twice, with its edges given each by the transposition of the initial entry of one such $2k$ -string with any entry that contains a different symbol than that of the initial entry. The pancake 2-set transposition graph PC_k^2 has the same vertex set of ST_k^2 and its edges involving each the maximal product of concentric disjoint transpositions in any prefix of an endvertex string, including the external transposition being that of an edge of ST_k^2 . For $1 < k \in \mathbb{Z}$, we show that ST_k^2 and PC_k^2 , among other intermediate transposition graphs, have total colorings via $2k - 1$ colors. They, in turn, yield efficient dominating sets, or E-sets, of the vertex sets of ST_k^2 and PC_k^2 , and partitions into into $2k - 1$ such E-sets, generalizing Dejter-Serra work on E-sets in such graphs.

Keywords: Total coloring, Efficient domination, Vertex-transitive graphs

2020 Mathematics Subject Classification: 05C15, 05C69, 05E18

1. Efficient Domination and Total Coloring of Graphs

Let $0 < k \in \mathbb{Z}$. Given a finite graph $G = (V(G), E(G))$ and a subset $S \subseteq V(G)$, it is said that S is an *efficient dominating set* (E-set) [1, 3, 2, 6, 7, 10] or a *perfect code* [4, 5], if for each $v \in V(G) \setminus S$ there exists exactly one vertex v^0 in S such that v is adjacent to v^0 .

Applications of E-sets occur in: **(a)** the theory of error-correcting codes and **(b)** estab-

✉ Corresponding author.

E-mail addresses: italo.dejter@gmail.com (Italo J. Dejter).

Received 18 March 2024; accepted 25 November 2024; published 31 December 2024.

DOI: [10.61091/ars161-06](https://doi.org/10.61091/ars161-06)

© 2024 The Author(s). Published by Combinatorial Press. This is an open access article under the CC BY license (<https://creativecommons.org/licenses/by/4.0/>).

lishing the existence of regular graphs for Network Theory by removing E-sets from their containing graphs.

A *total coloring* of a graph G is an assignment of colors to the vertices and edges of G such that no two incident or adjacent elements (vertices or edges) are assigned the same color [8]. A total coloring of G such that the vertices adjacent to each $v \in V(G)$ together with v itself are assigned pairwise different colors will be said to be an *efficient coloring*. The efficient coloring will be said to be *totally efficient* if G is k -regular, the color set is $[k] = \{0, 1, \dots, k-1\}$ and each $v \in V(G)$ together with its neighbors are assigned all the colors in $[k]$. The *total* (resp. *efficient*) *chromatic number* $\chi''(G)$ (resp. $\chi'''(G)$) of G is defined as the least number of colors required by a total (resp. efficient) coloring of G .

As for applications other than (a)-(b) above, note that: **(c)** by removing the vertices of a fixed color, then again regular graphs for Network Theory are generated; **(d)** by removing the edges of a fixed color, then copies of a non-bipartite biregular graph whose parts have vertices with degrees differing in a unit are determined, again applicable in Network Theory.

In Section 3, we show that the graphs of a family of graphs $G = ST_k^2$, ($0 < k \in \mathbb{Z}$), introduced in Section 2, satisfy the conditions of the following theorem. We conjecture that those conditions are only satisfied by such graphs $G = ST_k^2$, and not any other graphs.

Theorem 1.1. **(I)** *Let $3 < h \in 2\mathbb{Z}$. Let G be a connected $(h-2)$ -regular graph with a totally efficient coloring via color set $[h] \setminus \{0\} = \{1, \dots, h-1\}$. Then, there is a partition of V into $h-1$ subsets W_1, \dots, W_{h-1} , where W_i is formed by those vertices of G having color i , for each $i \in [h] \setminus \{0\}$. In such a case, $\chi'''(G) = h-1$. Moreover, each W_i is an E-set of G , for $i \in [h] \setminus \{0\}$. **(II)** *Let $4 < h \in 2\mathbb{Z}$. Then, $G \setminus W_i$ is a connected $(h-3)$ -regular subgraph that still has efficient chromatic number $h-1$, i.e. $\chi'''(G \setminus W_i) = h-1$, even though it has only a (non-total) efficient coloring. Letting E_i be the set of edges with color i in $G \setminus W_i$, then:**

- (a) $G \setminus W_i \setminus E_i$ is the disjoint union of copies of regular subgraphs of degree $h-4$ with efficient colorings by $h-3$ colors obtained from $[h] \setminus \{0, i\}$ by removing the edges of a color $j \neq i$;
- (b) $G \setminus E_i$ is a non-bipartite $(h-2, h-3)$ -biregular graph.

Proof. We use the inequality $\chi''(G) \geq \Delta(G)+1$, where $\Delta(G)$ is the maximum degree of G [8]. In our case, $\chi'''(G) = \chi''(G) = \Delta(G) + 1$. Because of this, a totally efficient coloring here provides a partition W_1, \dots, W_{h-2} as claimed in item (I). By definition of totally efficient coloring, each W_i is an E-set. For item (II), deleting W_i from G removes also all the edges incident to the vertices of W_i , so $G \setminus W_i$ still has an efficient coloring which is not totally efficient since there is an edge color lacking incidence to each particular vertex of $G \setminus W_i$. To establish item (II)1, note that removal of E_i from $G \setminus W_i$ for $h > 4$, leaves us with the graph induced by the edges of all colors other than color i , which necessarily disconnects $G \setminus W_i$, again because of the definition of totally effective coloring. To establish item (II)2, the removal of the edges with color i leaves their endvertices with

degree $h - 3$ and forming a vertex subset of the resulting $G \setminus E_i$, while the remaining vertices have color i , degree $h - 2$ and form a stable vertex set. This completes the proof of the theorem. All of this can be verified without loss of generality via the proof of Theorem 3.1, for $h = 2k$. \square

Let $\ell \in \{0, 1\}$. In Section 5, we generalize via ℓ -set permutations, (see Section 2), the result of [6] that the star transposition graphs form a *dense segmental neighborly E-chain*. In Section 6, we generalize star transposition graphs to pancake transposition graphs and related intermediate graphs [6], leading to an adequate version of dense neighborly E-chain [6], with obstructions preventing any convenient version of segmental E-chain [6].

2. Families of Multiset Transposition Graphs with E-Sets

Let $0 < \ell \in \mathbb{Z}$ and let $1 < k \in \mathbb{Z}$. We say that a string over the alphabet $[k]$ that contains exactly ℓ occurrences of i , for each $i \in [k]$, is an ℓ -set permutation. In denoting specific ℓ -set permutations, commas and brackets are often omitted.

Let V_k^ℓ be the set of all ℓ -set permutations of length $k\ell$. Let the *star ℓ -set transposition graph* ST_k^ℓ be the graph on vertex set V_k^ℓ with an edge between each two vertices $v = v_0v_1 \cdots v_{k\ell-1}$ and $w = w_0w_1 \cdots w_{k\ell-1}$ that differ in a *star transposition*, i.e. by swapping the first entry v_0 of $v = v_0v_1 \cdots v_{k\ell-1} \in V_k^\ell$ with any entry v_j ($j \in [k\ell] \setminus \{0\}$) whose value differs from that of v_0 (so $v_j \neq v_0$), thus obtaining either $w = w_0 \cdots w_j \cdots w_{k\ell-1} = v_j \cdots v_0 \cdots w_{k\ell-1}$ or $w = w_0 \cdots w_{k\ell-1} = v_{k\ell-1} \cdots v_0$. In other words, each edge of ST_k^ℓ is given by the transposition of the initial entry of an endvertex string with an entry that contains a different symbol than that of the initial entry. The graphs ST_k^ℓ are a particular case of the graphs treated in [9] in a context of determination of Hamilton cycles.

It is known that all k -permutations, (that is all 1-set permutations of length k), form the *symmetric group*, denoted Sym_k , under composition of k -permutations, each k -permutation $v_0v_1 \cdots v_{k-1}$ taken as a bijection from the *identity* k -permutation $01 \cdots (k-1)$ onto $v_0v_1 \cdots v_{k-1}$ itself. A graph ST_k^1 with $k > 1$ (which excludes ST_1^1) is the Cayley graph of Sym_k with respect to the set of transpositions $\{(0 i); i \in [k] \setminus \{0\}\}$. Such a graph is denoted ST_k in [1, 6], where is proven its vertex set admits a partition into k E-sets, exemplified on the left of Figure 1 for $ST_3^1 = ST_3$, with the vertex parts of the partition differentially colored in black, red and green, for respective first entries 0, 1 and 2. Figure 1 of [6] shows a similar example for $ST_4^1 = ST_4$. Also, the graph ST_k^ℓ is vertex transitive, but is neither a Cayley graph nor a Shreier graph; see Subsection 5.1, below.

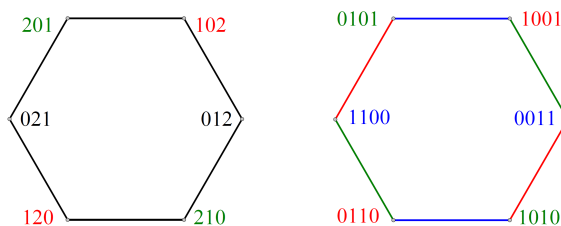


Fig. 1. The 6-cycles $ST_3^1 = ST_3$ and ST_3^2

3. E-sets of Star 2-set Transposition Graphs

Let $i \in [2k] \setminus \{0\} = \{1, \dots, 2k-1\}$. Let Σ_i^k be the set of vertices $v_0 v_1 \cdots v_{k-1}$ of ST_k^ℓ such that $v_0 = v_i$, ($i = 1, \dots, 2k-1$). Let E_i^k be the set of edges having color i in $G \setminus \Sigma_i^k$. We will show that Σ_i^k is an E-set of ST_k^2 . Clearly, no edge of E_i^k is incident to the vertices of Σ_i^k .

Theorem 3.1. *Let $k > 1$. (I) The graph ST_k^2 has $\frac{(2k)!}{2^k}$ vertices and regular degree $2(k-1)$. (II) Let $i \in [2k] \setminus \{0\} = \{1, \dots, 2k-1\}$ and let Σ_i^k be the set of vertices $v_0 v_1 \cdots v_{2k-1}$ of ST_k^2 such that $v_0 = v_i$. Then, V_k^2 admits a vertex partition into $2k-1$ E-sets Σ_i^k , ($i \in [2k] \setminus \{0\}$). (III) Let $k > 2$, let $j \in [2k] \setminus \{0\}$ and let E_j^k be the set of all edges of color j . Then, $ST_k^2 \setminus \Sigma_i^k \setminus E_i^k$ is the disjoint union of $k^2 k - 1$ copies of ST_{k-1}^2 .*

Proof. Let $i = 2k-1$ and let $j \in [2k]$. Then, each vertex $v = v_0 v_1 \cdots v_{2k-3} v_{2k-2} v_{2k-1} = 0v_1 \cdots v_{2k-3} j 0$ is the neighbor of vertex $w = j v_1 \cdots v_{2k-3} 0 0$ via an edge of color $k-1$. But $v \in \Sigma_i^k = \Sigma_{2k-1}^k$. Being w at distance 1 from Σ_{2k-1}^k , then w is in the open neighborhood $N(\Sigma_i^k)$ [6] of Σ_{2k-1}^k in ST_k^2 , so $w \in N(\Sigma_i^k) = N(\Sigma_{2k-1}^k) \subseteq ST_k^2 \setminus \Sigma_i^k \setminus E_i^k = ST_k^2 \setminus \Sigma_{2k-1}^k \setminus E_{2k-1}^k$. In fact, $N(\Sigma_i^k) = N(\Sigma_{2k-1}^k)$ is a connected component of $ST_k^2 \setminus \Sigma_i^k \setminus E_i^k = ST_k^2 \setminus \Sigma_{2k-1}^k \setminus E_{2k-1}^k$. A similar conclusion holds for each other open neighborhoods $N(\Sigma_i^k)$, ($1 \leq i < 2k-1$). \square

Remark 3.2. The total coloring of ST_k^2 will be referred to as its *color structure*. The $k2^{k-1}$ copies of ST_{k-1}^2 in ST_k^2 whose disjoint union is $ST_k^2 \setminus \Sigma_i^k \setminus E_i^k$ inherit each a color structure that generalizes that of Examples 3.3-3.4, below, and is similar to the color structure of ST_{k-1}^2 .

Example 3.3. The graph ST_2^2 has the totally efficient coloring depicted on the right of Figure 1, where $\Sigma_1^2 = \{0011, 1100\}$ is color blue, as is $E_1^2 = \{(0101, 1001), (0110, 1010)\}$; $\Sigma_2^2 = \{0101, 1010\}$ is color green, as is $E_2^2 = \{(0110, 1100), (0011, 1001)\}$; $\Sigma_3^2 = \{0110, 1001\}$ is color red, as is $E_3^2 = \{(0011, 1010), (0101, 1100)\}$.

Example 3.4. The graph ST_3^2 has the E-set Σ_3^3 with 18 vertices denoted as in display (1):

$$\begin{cases} A = 011220, & \underline{A} = 022110, & B = 012210, & \underline{B} = 021120, & C = 012120, & \underline{C} = 021210, \\ D = 122001, & \underline{D} = 100221, & E = 120021, & \underline{E} = 102201, & F = 120201, & \underline{F} = 102021, \\ G = 200112, & \underline{G} = 211002, & H = 201102, & \underline{H} = 210012, & J = 201012, & \underline{J} = 210102. \end{cases} \quad (1)$$

A planar interconnected disposition of the 6-cycles of the subgraph $ST_3^2 \setminus \Sigma_3^3$ of ST_3^2 is shown in Figure 2. The edges of such 6-cycles are alternatively colored with 2 or 3 colors of the color form $(ababab)$ or $(abcabc)$ respectively, where $\{a, b, c\} \subseteq \{1, 2, 3, 4\}$ is a subset of colors provided by the respective positions 1,2,3,4 of the 6-tuples taken as the vertices of ST_3^2 .

The tessellation suggested in Figure 2 can be extended to the whole plane as an unfolding of the fundamental region delimited by the shown dash-border rectangle – call it R .

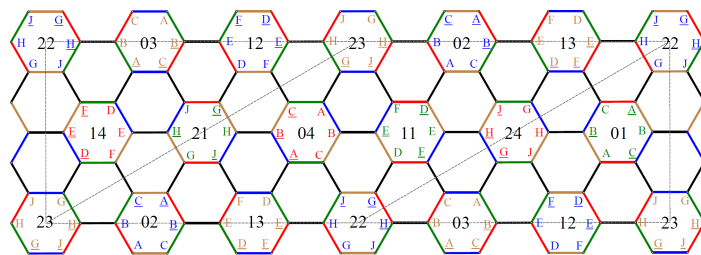


Fig. 2. A fundamental region of a lattice suggests a rhomboidal torus cutout of ST_3^2

This R appears partitioned via dashed segments into two right triangles and a rhomboid in between. By transporting the left right triangle – call it $T_l \subset R$ – to a new position T_l' to the right so that the vertical side of T_l' coincides with the right side of R , a rhomboid R' is obtained. Identification of the tilted sides of R' and of its horizontal sides allows to view a toroidal embedding of $ST_3^2 \setminus \Sigma_5^3$.

Edge colors in Figure 2 are numbered as follows (indicating corresponding subsequent positions in the 6-tuples representing the vertices of ST_3^2):

$$1 = \textit{green}, 2 = \textit{blue}, 3 = \textit{hazel}, 4 = \textit{red}, 5 = \textit{black}. \tag{2}$$

In Figure 2, the 3-colored 6-cycles are exactly those containing in their interiors (next to their corresponding denoting vertices) the (possibly underlined) capital letters of display (1), but each such letter colored as indicated in display (2). Each such number color $a \in \{1, 2, 3, 4\}$ as in display (2) of a symbol $X \in \{A, \dots, J, \underline{A}, \dots, \underline{J}\}$ in Figure 2 indicates the existence of an (absent) a -colored edge between $V_3^2 \setminus \Sigma_5^3$ and Σ_5^3 in ST_3^2 . Figure 3 shows each such edge in exactly one copy Υ of $K_{1,4}$ with its endvertex in Σ_5^3 represented by X (in black) and its other endvertex being the sole element of $\Upsilon \cap V_3^2 \setminus \Sigma_5^3$, namely the a -colored X , that we denote as X^a in Table 1. In fact, Table 1 reproduces the data of Figure 2 in a likewise disposition, with the vertex notation X^a instead of the a -colored X notation of Figure 2. In Table 1, edges are represented by their numeric symbols (display (2)) and appear interspersed with the symbols X^a in representing the 3-colored 6-cycles, while 2-colored 6-cycles are represented by the disposition of their numeric symbols. Note in Figure 2 that each 3-colored 6-cycle is bordered by six 2-colored 6-cycles via edges colored in $\{1, 2, 3, 4, \}$, while each 2-colored 6-cycle, call it Θ , is bordered by three 3-colored 6-cycles (via edges in one fixed color of $\{1, 2, 3, 4\}$) alternated with three 2-colored 6-cycles via an edge matching bordering Θ and whose color is 1.

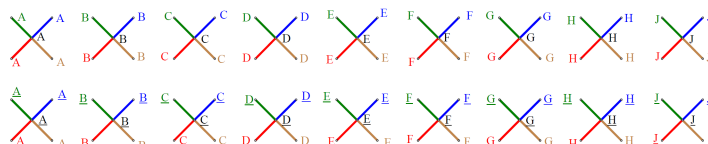


Fig. 3. The eighteen stars $K_{1,4}$ in ST_3^2 centered at the vertices of the E-set Σ_5^3

Table 2 represents the twelve 3-colored 6-cycles, as follows. The six centers $X \in \{A, \dots, J, \underline{A}, \dots, \underline{J}\}$ of copies of $K_{1,4}$ involved with one such 3-colored 6-cycle, call it Φ , are represented by 6-tuples that are expressed in Table 2 in a 6-row section of a

$1\underline{J}^23\underline{G}^24$	$4\underline{C}^32\underline{A}^31$	$1\underline{F}^23\underline{D}^24$	$4\underline{J}^32\underline{G}^31$	$1\underline{C}^23\underline{A}^24$	$4\underline{F}^32\underline{D}^31$
H^2	\underline{H}^2	5	B^3	\underline{B}^3	5
E^2	\underline{E}^2	5	H^3	\underline{H}^3	5
B^2	\underline{B}^2	5	E^3	\underline{E}^3	5
$4G^23J^21$	$1\underline{A}^32\underline{C}^34$	$4D^23F^21$	$1\underline{G}^32\underline{J}^34$	$4A^23C^21$	$1\underline{D}^32\underline{F}^34$
5	5	5	5	5	5
5	5	5	5	5	5
$3\underline{F}^41\underline{D}^42$	$2\underline{J}^44\underline{G}^43$	$3\underline{C}^41\underline{A}^42$	$2\underline{F}^44\underline{D}^43$	$3\underline{J}^41\underline{G}^42$	$2\underline{C}^44\underline{A}^43$
5	\underline{E}^4	E^4	5	\underline{H}^1	H^1
5	\underline{B}^4	B^4	5	\underline{E}^1	E^1
5	\underline{H}^4	H^4	5	\underline{B}^1	B^1
$2\underline{D}^41\underline{F}^43$	$3\underline{G}^44\underline{J}^42$	$2\underline{A}^41\underline{C}^43$	$3\underline{D}^44\underline{F}^42$	$2\underline{G}^41\underline{J}^43$	$3\underline{A}^44\underline{C}^42$
5	5	5	5	5	5
$4J^32G^32$	$1\underline{C}^23\underline{A}^24$	$4F^32D^31$	$1\underline{J}^23\underline{G}^24$	$4C^32A^31$	$1\underline{F}^23\underline{D}^24$
H^3	\underline{H}^3	5	B^2	\underline{B}^2	5
E^3	\underline{E}^3	5	H^2	\underline{H}^2	5
B^3	\underline{B}^3	5	E^2	\underline{E}^2	5
$1\underline{G}^32\underline{J}^34$	$4A^23C^21$	$1\underline{D}^32\underline{F}^34$	$4G^23J^21$	$1\underline{A}^32\underline{C}^34$	$4D^23F^21$
5	5	5	5	5	5

Table 1. Notational disposition of elements of ST_3^2 in Figure 2

column whose heading is Σ_5^3 . To the immediate right of each such 6-row section, another 6-row section of 6-tuples expresses the corresponding neighbors X^b , for a fixed color $b \in \{1, 2, 3, 4\}$, via b -colored edges. Such neighbors X^b conform $V(\Phi)$ and induce Φ . In fact, Table 2 contains the twelve instances of such representations.

Notice that the vertices in display (1) are of the form $ia_1a_2a_3a_4i$. Centered inside each 3-colored 6-cycle Φ in Figure 2, a pair (i, b) of digits (written as ib) indicates the fixed double entry $i \in \{0, 1, 2\}$ of the vertices $ia_1a_2a_3a_4i$ of Σ_5^3 in Φ and the fixed color b their representing symbols have in the figure.

To facilitate viewing the edge colors along each Φ , the second row in Table 2 shows the 6-tuple x of subsequent positions (or colors), 012345, of the 6-tuples representing each X and X^b . In each such x under the heading Σ_5^3 , the entry $b \in \{1, 2, 3, 4\}$ of the corresponding X^b is underlined, while under each subsequent heading X^b , the other three entries in $\{1, 2, 3, 4\}$ are underlined to indicate the entries successively transposed with the initial entry in the subsequent vertically disposed 6-tuples of each particular Φ .

Observe the difference between 3-colored 6-cycles appearing here and 2-colored 6-cycles in that the former are created by transpositions not involving the initial entry while the latter do involve transpositions with the initial entry.

In Figure 2, deletion of the edges colored 1 from $ST_3^2 \setminus \Sigma_5^3$ leaves a subgraph with twelve components, each being a 3-colored 6-cycle. Note that $E(ST_3^2)$ has a 1-factorization into five 1-factors $E_1^3, E_2^3, E_3^3, E_4^3, E_5^3$, each E_i^3 composed by those edges colored i , ($i \in [6] \setminus \{0\}$). Moreover, $ST_3^2 \setminus \Sigma_5^3 \setminus E_5^3$ is the union of the twelve 3-colored 6-cycles in Table 2.

Corollary 3.5. Let $k > 2$. Then:

- ST_k^2 has $\frac{2k!}{2^k}$ vertices having $\frac{2k!}{2^k(2k-1)}$ vertices in each color $1, 2, \dots, 2k-1$;
- ST_k^2 has $\frac{2k!}{2^k} \times (k-1)$ edges;
- color $k\ell-1$ provides exactly $\frac{2k!}{2^k(2k-1)} = y$ vertices forming a PDS Σ_{2k-1}^k of ST_k^2 ;

- (d) the y resulting dominating copies of $K_{1,2k-2}$ have a total of $y \times (2k - 2) = z$ edges;
- (e) there are exactly $\frac{2k!}{2^k} \times (k - 1) - z = h$ edges in ST_{2k-1}^k not counted in item 4;
- (f) the h edges in item 5. contain $\frac{h}{2k-1}$ edges in each color $1, 2, \dots, 2k - 1$;
- (g) so they contain $h - \frac{h}{2k-1}$ edges in colors $\neq 2k - 1$, (namely, $1, 2, \dots, 2k - 2$);
- (h) there are $\frac{2k!}{2^k} - y$ vertices in $ST_k^2 \setminus \Sigma_{2k-1}^k$ dominated by Σ_{2k-1}^k ;
- (i) the $\frac{2k!}{2^k} - y$ vertices in item 8. appear in $k \times (2k - 2)$ copies of ST_{k-1}^2 ;
- (j) there are $\frac{h}{(2k-1)2^k}$ edges in each copy of ST_{2k-1}^k in $ST_k^2 \setminus \Sigma_{2k-1}^k$.

X	Σ_5^3	X^1	X	Σ_5^3	X^2	X	Σ_5^3	X^3	X	Σ_5^3	X^4
x	012345	012345	x	012345	012345	x	012345	012345	x	012345	012345
A	011220	101220	A	011220	110220	A	011220	211020	A	011220	211200
\underline{B}	021120	201120	B	012210	210210	\underline{B}	021120	121020	B	012210	112200
C	012120	102120	\underline{C}	021210	120210	\underline{C}	021210	221010	C	012120	212100
\underline{A}	022110	202110	\underline{A}	022110	220110	\underline{A}	022110	122010	\underline{A}	022110	122100
B	012210	102210	\underline{B}	021120	120120	B	012210	212010	\underline{B}	021120	221100
\underline{C}	021210	201210	C	012120	210120	C	012120	112020	\underline{C}	021210	121200
D	122001	212001	D	122001	221001	D	122001	022101	D	122001	022011
\underline{E}	102201	012201	E	120021	021021	\underline{E}	102201	202101	E	120021	220011
F	120201	210201	\underline{F}	102021	201021	\underline{F}	102021	002121	F	120201	020211
\underline{D}	100221	010221	\underline{D}	100221	001221	\underline{D}	100221	200121	\underline{D}	100221	200211
E	120021	210021	\underline{E}	102201	201201	E	120021	020121	\underline{E}	102201	002211
\underline{F}	102021	012021	F	120201	021201	F	120201	220101	\underline{F}	102021	202011
G	200112	020112	G	200112	002112	G	200112	100212	G	200112	100122
\underline{H}	210012	120012	H	201102	102102	\underline{H}	210012	010212	H	201102	001122
J	201012	021012	\underline{J}	210102	012102	\underline{J}	210102	110202	J	201012	101022
\underline{G}	211002	121002	\underline{G}	211002	112002	\underline{G}	211002	011202	\underline{G}	211002	011022
H	201102	021102	\underline{H}	210012	012012	H	201102	101202	\underline{H}	210012	110022
\underline{J}	210102	120102	J	201012	102012	\underline{J}	210102	001212	\underline{J}	210102	010122

Table 2. The twelve 6-cycles whose vertices start with 00, 11 and 22

Proof. The ten items of the corollary can be verified directly from the enumerative facts involved with the graphs ST_k^2 . □

Example 3.6. For ST_3^2 , we have that:

- (a) ST_3^2 has $\frac{6!}{2^3} = 90$ vertices containing $\frac{90}{5} = 18$ vertices in each color $1, 2, 3, 4, 5$;
- (b) ST_3^2 has $90 \times 4/2 = 180$ edges;
- (c) color 5 provides 18 vertices that form a PDS Σ_5^3 of ST_3^2 ;

- (d) the 18 resulting dominating copies of $K_{1,4}$ in ST_3^2 have $18 \times 4 = 72$ edges;
- (e) outside that, there are still $180 - 72 = 108$ edges;
- (f) they contain $\frac{108}{5} = 36$ edges in each color 1, 2, 3, 4, 5;
- (g) so they contain $108 - 36 = 72$ edges in colors $\neq 5$, (namely, 1, 2, 3, 4);
- (h) there are $90 - 18 = 72$ remaining vertices in ST_3^2 , dominated by Σ_5^3 ;
- (i) they appear in $3 \times 4 = 12$ copies of ST_2^2 ;
- (j) there are $\frac{72}{3 \times 4} = \frac{72}{12} = 6$ edges in each copy of ST_2^2 in $ST_3^2 \setminus \Sigma_5^3$.

Example 3.7. For ST_4^2 , we have that:

- (a) ST_4^2 has $\frac{8!}{2^4} = 2520$ vertices containing $\frac{2520}{7} = 360$ vertices in each color 1, ..., 7;
- (b) ST_4^2 has $2520 \times 6/2 = 7560$ edges;
- (c) color 7 provides 360 vertices that form a PDS Σ_7^4 of ST_4^2 ;
- (d) the 360 resulting dominating copies of $K_{1,6}$ in ST_4^2 have $360 \times 6 = 2160$ edges;
- (e) outside that, there are still $7560 - 2160 = 5400$ edges;
- (f) they contain $\frac{5400}{7} = 1080$ edges in each color 1, 2, 3, 4, 5, 6, 7;
- (g) the h edges in item 6 have $5040 - 1080 = 4320$ edges in colors $\neq 7$, (namely, 1, ..., 6);
- (h) there are $2520 - 360 = 2160$ remaining vertices in ST_4^2 , dominated by Σ_7^4 ;
- (i) they appear in $4 \times 6 = 24$ copies of ST_3^2 ;
- (j) there are $\frac{4320}{4 \times 6} = \frac{4320}{24} = 180$ edges in each copy of ST_3^2 in $ST_4^2 \setminus \Sigma_7^4$.

Example 3.8. The 24 copies of ST_3^2 in ST_4^2 , (item 5 of Example 3.7), can be encoded as follows. We start by encoding the fundamental rectangle in Figure 2 by arranging the pairs $(i, b) = ib$ as follows, following the disposition in the figure:

$$\begin{array}{cccccccc}
 22 & 03 & 12 & 23 & 02 & 13 & 22 & \\
 & 14 & 21 & 04 & 11 & 24 & 01 & \\
 23 & 02 & 13 & 22 & 03 & 12 & 22 &
 \end{array} \tag{3}$$

By further encoding this disposition as (012, 1234), we now have that the 24 copies of ST_3^2 in ST_4^2 can be expressed as:

$$(123, 123456), (013, 123456), (023, 123456), (012, 123456).$$

A characterization of the twenty-four 2-colored 6-cycles of $ST_3^2 \setminus \Sigma_1^3$ is also available from that of the twelve 3-colored 6-cycles in display (3). Let us observe the triple $(0x_0, 1y_1, 2y_2)$ formed by the three pairs $0x_0, 1x_1, 2x_2$ denoting the three 3-colored 6-cycles that share each an edge e with a given 2-colored 6-cycle Θ_e . By shortening each such triple of pairs to the triple of colors $x_0x_1x_2$ and setting its missing color x_3 in $\{1, 2, 3, 4\}$ as a subindex,

with colors $i = 5$ and x_3 assigned alternatively to the edges of each Θ_e , we have now the disposition in display (4) which is similar to that of Figure 2:

$$\begin{array}{cccccccccccc}
 22 & & 03 & & 12 & & 23 & & 02 & & 13 & & 22 \\
 142_3 & 342_1 & 341_2 & 321_4 & 421_3 & 423_1 & 413_2 & 213_4 & 214_3 & 234_1 & 134_2 & 132_4 & 142_3 \\
 & & 14 & & 21 & & 04 & & 11 & & 24 & & 01 \\
 143_2 & 243_1 & 241_3 & 231_4 & 431_2 & 432_1 & 412_3 & 312_4 & 314_2 & 324_1 & 124_3 & 123_4 & 143_2 \\
 23 & & 02 & & 13 & & 22 & & 03 & & 12 & & 23
 \end{array} \tag{4}$$

Again, this disposition is encoded as (123, 1234).

Theorem 3.9. *The graphs ST_k^2 satisfy the conditions of Theorem 1.1, so they also satisfy its conclusions.*

Proof. Because of the previous discussion, we see that in the hypotheses of Theorem 1.1 it is enough to take $h = 2k$, $G = ST_k^2$, $W_i = \Sigma_i^k$ and $E_i = E_i^k$. □

4. Open Problems

We conjectured that the graph G in the statement of Theorem 1.1 must necessarily coincide with some ST_k^2 . On the other hand, the twenty-four 2-colored 6-cycles of $ST_3^2 \setminus \Sigma_5^3$ generalize to 2-colored 6-cycles in $ST_k^2 \setminus \Sigma_{2k-1}^k$, for any $k > 3$, by similarly alternating three black edges (meaning color $2k - 1$) with three edges of a common color different from $2k - 1$ in order to obtain one such 2-colored 6-cycle. Performing this to include all edges of $ST_k^2 \setminus \Sigma_{2k-1}^k$, still we do not know how to generalize for $k > 3$ what happens between the $k2^{k-1}$ copies of ST_{k-1}^2 in Theorem 3.1 and the black edges (colored via $2k - 1$). The determination of this particular matter is left as an open problem.

As a hint to illuminate the problem, let us recall that ST_k^2 has $\frac{(2k)!}{2^k}$ vertices and regular degree $2(k - 1)$; then it has $\frac{(2k)!(k-1)}{2^k}$ edges and a total coloring via $2k - 1$ colors. The number of vertices in ST_k^2 having a fixed color is $\frac{(2k)!}{2^k(2k-1)}$. The copies of stars $K_{1,2k-2}$ with centers on vertices of ST_k^2 having a fixed color contain a total of $\frac{(2k)!(2k-2)}{2^k(2k-1)} = \frac{2k!(k-1)}{2^{k-1}(2k-1)}$ edges. The numbers of remaining vertices and edges, namely those of $ST_k^2 \setminus \Sigma_{2k-1}^k$, are $\frac{(2k)!}{2^k} - \frac{(2k)!}{2^k(2k-1)}$ and $\frac{(2k)!(2k-1)}{2^k} - \frac{(2k)!(k-1)}{2^{k-1}(2k-1)}$, respectively. The edges of $ST_k^2 \setminus \Sigma_{2k-1}^k$ with a fixed color are divided into groups of three edges, each such group with alternate edges of a corresponding 2-colored 6-cycle, with the other three alternating edges in color $2k - 1$. A conclusion here is that the number of 2-colored 6-cycles must be the third part of $\frac{(2k)!(2k-1)}{2^k} - \frac{(2k)!(k-1)}{2^{k-1}(2k-1)}$, which for $k = 3$ equals 24, as can be counted for example via Figure 2.

5. Conclusions for Star 2-set Transposition Graphs

Let us recall from [6] that:

- (a) a countable family of graphs

$$\mathcal{G} = \{\Gamma_1 \subset \Gamma_2 \subset \dots \subset \Gamma_i \subset \Gamma_{i+1} \subset \dots\},$$

is said to be an *E-chain* if every Γ_i is an induced subgraph of Γ_{i+1} and each Γ_i has an E-set C_i ;

- (b) for graphs Γ and Γ' , a one-to-one graph homomorphism $\zeta : \Gamma \rightarrow \Gamma'$ such that $\zeta(\Gamma)$ is an induced subgraph of Γ' is said to be an *inclusive map*;
- (c) for $i \geq 1$, let κ_i be an inclusive map of Γ_i into Γ_{i+1} ; if $C_{i+1} = N(\kappa_i(V(\Gamma_i)))$, then the E-chain \mathcal{G} is said to be a *neighborly E-chain*;
- (d) a particular case of E-chain \mathcal{G} is the one in which C_{i+1} has a partition into images $\zeta_i^{(j)}(C_i)$ of C_i through respective inclusive maps $\zeta_i^{(j)}$, where j varies on a suitable finite indexing set. In such a case, the E-chain is said to be *segmental*.

The notion of neighborly E-chain in item 3 above is not suitable in our context of graphs ST_k^2 and their E-sets, that we denote Σ_{2k-1}^k (instead of C_i as in [6]), like Σ_3^2 and Σ_5^3 in Example 3.4, with Σ_5^3 detailed both in display (1) and Figures 2-3, and also in Tables 1-2. In this context, the graphs ST_k^2 form an E-chain

$$\mathcal{ST}(2) = \{ST_1^2 \subset ST_2^2 \subset \dots \subset ST_k^2 \subset ST_{k+1}^2 \subset \dots\}, \quad (5)$$

with each inclusion $ST_k^2 \subset ST_{k+1}^2$ realized by a set of $k+1$ *neighborly maps*

$$\kappa_k^j : ST_k^2 \rightarrow ST_{k+1}^2, \quad (6)$$

($j \in [k+1]$), (*neighborly* meaning that the images $\kappa_k^j(ST_i^2)$ are pairwise disjoint in ST_{k+1}^2 and that

$$\Sigma_k^{k+1} = \cup_{j=1}^{k-1} N(\kappa_i^j(V_i^2)), \quad (7)$$

as a disjoint union), these neighborly maps given by

$$\kappa_k^j(a_0 a_1 \dots a_{2k-2} a_{2k-1}) = (a_0^j a_1^j \dots a_{2k-2}^j a_{2k-1}^j j j), \quad (8)$$

for $j \in [k+1]$, where

$$a_i^k = a_i, a_i^{k+1} = a_i + 1 \pmod{(k+1)}, \dots, a_i^{k+h} = a_i + h \pmod{(k+1)}, \dots, \quad (9)$$

for $i = 0.1, \dots, 2k-1$, the superindices $k+h$ of the entries a_i^{k+h} taken mod $k+1$.

As an example, the last column of Table 2 offers disjoint neighborly maps κ_2^j , for $j = 0, 1, 2$, yielding respectively the following images of the 6-cycle that comprises ST_2^2 :

$$\begin{aligned} \kappa_2^2(1001, 0011, 1010, 0110, 1100, 0101) &= (100122, 001122, 101022, 011022, 110022, 010122); \\ \kappa_2^0(1001, 0011, 1010, 0110, 1100, 0101) &= (211200, 112200, 212100, 122100, 221100, 121200); \\ \kappa_2^1(1001, 0011, 1010, 0110, 1100, 0101) &= (022011, 220011, 020211, 200211, 002211, 202011). \end{aligned}$$

An E-chain as in display (5) where each inclusion $ST_k^2 \subset ST_{k+1}^2$ is realized by $k+1$ neighborly maps κ_k^j , as defined in displays (6) to (9), is said to be a *disjoint neighborly E-chain*.

The notion of segmental E-chain can also be generalized to the case of the graphs ST_k^2 , where in item 3 above we replace "neighborly" by "disjoint neighborly". In that case, the

E-chain will be said to be *disjoint segmental*. It is clear by symmetry that the E-chain $\mathcal{ST}(2)$ of display (5) is disjoint segmental, as exemplified via Figures 2 and 3 and the related Tables 1 and 2.

If, for each $i \geq 1$, there exists an inclusive map $\zeta_i : \Gamma_i \rightarrow \Gamma_{i+1}$ such that $\zeta(C_i) \subset C_{i+1}$, then [6] calls the E-chain *inclusive* and observes that an inclusive neighborly E-chain has $\kappa_i \neq \zeta_i$, for every positive integer i .

5.1. Density

In addition, [6] calls an E-chain \mathcal{G} *dense* if, for each $n \geq 1$, one has $|V(\Gamma_n)| = (n + 1)!$ and $|C_n| = n!$. However, this notion is not helpful in our present context.

For $k > 1$, note that $ST_{k\ell}^1$ is the Cayley graph of $Sym_{k\ell}$ generated by the transpositions $(0 i)$, $(0 < i < k\ell)$, but that ST_k^ℓ is not even a Shreier coset graph of the quotient of $Sym_{k\ell}$ modulo say its subgroup H_ℓ generated by the transpositions $(a a + 1)$, $(0 \leq a < k)$, because the edges of ST_k^ℓ are not given by transpositions $(0 i)$ independently of the values i in different vertices of ST_k^ℓ . However, Table 3 do generalize for every ST_k^2 , $(k \geq 2)$, where the table shows vertically:

- (a) the right cosets of V_4^1 mod the subgroup generated by transpositions $(0 1), (2 3)$;
- (b) the representations of such right cosets as vertices of ST_2^2 ; and
- (c) assigned generating sets of transpositions $(0 i)$ per shown right coset of V_3^1 or its representing vertex in ST_2^2 .

Right cosets of $V_4^1 \text{ mod } H$	0123	2301	0213	2031	0231	2013
	0132	2310	0312	2130	0321	2103
	1023	3201	1203	3021	1230	3012
	1032	3210	1302	3120	1320	3102
V_2^2	0011	1100	0101	1010	0110	1001
Gnr. set	$(0 2), (0 3)$	$(0 2), (0 3)$	$(0 1), (0 3)$	$(0 1), (0 3)$	$(0 1), (0 2)$	$(0 1), (0 2)$

Table 3. The right cosets of V_4^1 as the vertices of ST_2^2 and their generating sets

Tables like Table 3, but for $k > 2$, suggest extending the definition of a Shreier coset graph as follows: A *Shreier local coset graph* of a group G , a subgroup H of G and a generating set $S(Hg)$ for each right coset Hg of H in G , is a graph whose vertices are the right cosets Hg and whose edges are of the form (Hg, Hgs) , for $g \in G$ and $s \in S(Hg)$. The example in display (3) shows that ST_2^2 is a Shreier local coset graph of the group V_4^1 , its subgroup H generated by the transpositions $(0 1)$ and $(2 3)$, and the local generators indicated in the last line of the display. In a similar way, it can be shown for $k > 2$ that ST_k^2 is a Shreier local coset graph of V_k^2 with respect to its subgroup generated by the transpositions $(2a 2a + 1)$ with $0 \leq a < k$. Now, the density observed in [6] must be replaced to be useful in the present context of 2-set star transposition graphs. It is clear that in this sense, the E-sets found in the graphs ST_k^2 in Section 3 are as dense as they can be, so we say that these E-sets are *2-dense*. Then, the final conclusion of the present section is the following result.

Theorem 5.1. *The E-chain $\mathcal{ST}(2)$ of display (5) is a 2-dense, disjoint segmental, disjoint neighborly E-chain via the E-sets Σ_i^k of Theorem 3.1.*

Proof. The discussion above in this Section 5 provides all the properties in the statement. \square

6. Pancake 2-set Transposition Graphs

Let π_i be an arbitrary product of independent transpositions on the set $\{1, \dots, i-1\}$, ($i > 1$), where π_1 and π_2 are the identity. For each integer $k \geq 1$, let

$$A(\pi_1, \dots, \pi_i, \dots, \pi_{2k-1}) = \{(0\ 1)\pi_1, \dots, (0\ i)\pi_i, \dots, (0\ (2k-1))\pi_{2k-1}\}.$$

Lemma 2 of [6] implies that for $k \geq 1$ and any choice of the involutions π_i , ($i \geq 3$), the set $A(\pi_1, \dots, \pi_{2k-1})$ generates Sym_{2k-1} . For each choice of involutions π_1, π_2, \dots , the sequence of Cayley graphs with generating set $A(\pi_1, \dots, \pi_{2k-1})$ forms a chain of nested graphs with natural inclusions $\Gamma_k \subset \Gamma_{k+1}$.

Let $\ell \in \{1, 2\}$. If we choose the identity for each entry in $A(\pi_1, \dots, \pi_{2k-1})$, then we get the ℓ -set star transposition graphs ST_k^ℓ . If $\pi_i = (1\ (i-1)) \cdots ([i/2]\ [i/2])$, for $i = 3, \dots, k-1$, then we get the *pancake ℓ -set transposition graph* PC_k^ℓ . In particular, the pancake 2-set transposition graph PC_k^2 has the same vertex set of ST_k^2 and its edges involve each the maximal product of concentric disjoint transpositions in any prefix of an endvertex string, including the external transposition being that of an edge of ST_k^2 . The graphs PC_k^1 were seen in [6] to form a dense segmental neighborly E-chain $\mathcal{PC}(1) = \{PC_1^1, PC_2^1, \dots, PC_k^1, \dots\}$. (Figure 2 of [6] represents the graph PC_4^1). In a similar fashion to that of Section 5, the following partial extension of that result can be established.

Theorem 6.1. *The chain $\mathcal{PC}(2) = \{PC_1^2, PC_2^2, \dots, PC_k^2, \dots\}$ is a 2-dense, disjoint neighborly E-chain via the E-sets Σ_{2k-1}^k of Theorem 3.1, but it fails to be disjoint segmental. A similar result is obtained for any choice of the involutions $\pi_1, \pi_2, \dots, \pi_i \dots$ with not all the π_i s being identity permutations.*

Proof. Adapting the arguments given for star 2-set transposition graphs in Section 5 can only be done for the E-sets Σ_{2k-1}^k in pancake 2-set transposition graphs, since the feasibility for the sets Σ_i^k , ($1 \leq i < 2k-1$), to be E-sets is obstructed by the pancake transpositions in $A(\pi_1, \dots, \pi_{2k-1})$, meaning that we can only establish that the E-chain $\mathcal{PC}(2)$ is dense and disjoint neighborly, but not disjoint segmental. The "black" vertices, those whose color is $2k-1$, form an E-set Σ_{2k-1}^k with the desired properties, and their removal leaves a $2k-2$ -regular graph from which the removal of the "black" edges, forming an edge subset E_{2k-1}^k , leaves the disjoint union of the open neighborhoods $N(v)$ of the vertices v in the E-set Σ_{2k-1}^k . This behavior is similar for any other choice of the involutions $\pi_1, \pi_2, \dots, \pi_i \dots$ with not all the π_i s being identity permutations, other than $\pi_i = (1\ (i-1)) \cdots ([i/2]\ [i/2])$, for $i = 3, \dots, k-1$, which were used precisely to define the pancake graphs. \square

References

- [1] S. Arumugam and R. Kala. Domination parameters of star graph. *Ars Combinatoria*, 44:93–96, 1996.
- [2] D. W. Bange, A. E. Barkausas, L. H. Host, and P. J. Slater. Generalized domination and efficient domination in graphs. *Discrete Mathematics*, 159:1–11, 1996. [https://doi.org/10.1016/0012-365X\(95\)00094-D](https://doi.org/10.1016/0012-365X(95)00094-D).
- [3] D. W. Bange, A. E. Barkausas, and P. J. Slater. Efficient dominating sets in graphs. In R. D. Ringeisen and F. S. Roberts, editors, *Applications of Discrete Math*. Pages 189–199. SIAM, Philadelphia, 1988.
- [4] J. Borges and J. Rifá. A characterization of 1-perfect additive codes. *IEEE Transactions on Information Theory*, 46:1688–1697, 1999. <https://doi.org/10.1109/18.771247>.
- [5] I. J. Dejter. Sqs-graphs of extended 1-perfect codes. *Congressus Numerantium*, 193:175–194, 2008.
- [6] I. J. Dejter and O. Serra. Efficient dominating sets in cayley graphs. *Discrete Applied Mathematics*, 129:319–328, 2003. [https://doi.org/10.1016/S0166-218X\(02\)00573-5](https://doi.org/10.1016/S0166-218X(02)00573-5).
- [7] I. J. Dejter and O. Tomaiconza. Nonexistence of efficient dominating sets in the cayley graphs generated by transposition trees of diameter 3. *Discrete Applied Mathematics*, 232:116–124, 2017. <https://doi.org/10.1016/j.dam.2017.07.013>.
- [8] J. Geetha, N. Narayanan, and K. Somasundaram. Total coloring-a survey. *AKCE International Journal of Graphs and Combinatorics*, 20(3):339–351, 2023. <https://doi.org/10.1080/09728600.2023.2187960>.
- [9] P. Gregor, A. Merino, and T. Mütze. Star transpositions gray codes for multiset permutations. *Journal of Graph Theory*, 103(2):212–270, 2023. <https://doi.org/10.1002/jgt.22915>.
- [10] T. W. Haynes, S. T. Hedetniemi, and M. A. Henning. Efficient domination in graphs. In *Domination in Graphs: Core Concepts*, Springer Monographs in Mathematics, pages 259–289. Springer, 2023. https://doi.org/10.1007/978-3-031-09496-5_9.